# Mechanism of Interchange of the Syn and Anti Protons of Tetra(*trihapto*allyl)zirconium(IV)[1]

JEANNE K. KRIEGER,[2] J. M. DEUTCH, and GEORGE M. WHITESIDES*

The temperature dependence of the $^1$H nmr spectrum of tetra(*trihapto*allyl)zirconium(IV) (**5**) in CFCl$_3$ solution demonstrates that the syn and anti protons of the allyl moieties interchange. The experimental spectra of the central proton (H$_1$) of the allyl group were compared with line shapes calculated assuming two limiting types of interchange schemes: one (a "concerted" scheme, eq 3) in which interchange occurs simultaneously at the two ends of the allyl group and a second (called a "$\sigma,\pi$" scheme, eq 1) in which interchange occurs at one end of the allyl group at a time. The latter scheme leads to calculated spectra in good agreement with the experimental spectra; the former does not. Calculations performed at several levels of completeness were compared in an effort to identify qualitatively those spectral parameters required to obtain agreement between calculated and observed spectra, in the relatively complex coupled spin system provided by **5**. A very simple classical description utilizing only large coupling constants is capable of describing all of the features of the spectrum qualitatively; however, inclusion of small couplings is required for generation of calculated spectra in quantitative agreement with observed spectra. Although the classical description cannot be used for final spectral refinement, it nonetheless provides a comprehensible picture of the physical processes underlying the dynamic line shape behavior of **5**.

## Introduction

The occurrence of reactions resulting in the interchange of syn and anti hydrogens of *trihapto*allylmetal complexes is widespread, and these reactions have been extensively studied using dynamic nuclear magnetic resonance spectroscopic techniques.[3] Three basic classes of mechanisms have been proposed for these interchange reactions. The first consists of transformation of the *trihapto*allyl moiety (**1**) to a *monohapto*allyl group (**2**), rotation within **2** through 180° around the CH-CH$_2$M carbon–carbon single bond, and reversion to a *trihapto*allyl complex (eq 1). The second requires equilibration of **1** with a 1,2-*dihapto*allyl complex (**3**), rapid rotation around the carbon–carbon bond connecting the coordinated vinyl group with the unattached methylene group (eq 2), and return to **1**. The third consists of isomerization of **1** to a 1,3-*dihapto*allyl complex having the three carbon atoms of the allyl group and the metal atom in a common plane, followed by return to **1** (eq 3).



$$(1)$$



$$(2)$$



$$(3)$$
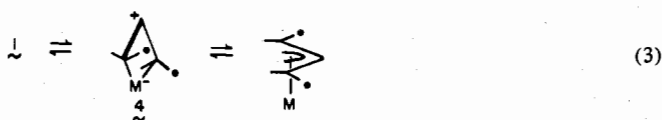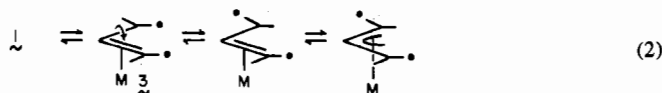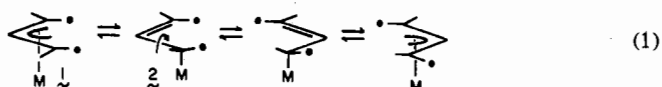
Nmr studies of the influence of added ligands on the rates of syn–anti interchange and of the influence of chiral ligands on the spectral changes characterizing the *trihapto*allyl

moiety in the region of intermediate interchange rates have firmly established the first mechanism (eq 1, hereafter referred to as the "$\sigma,\pi$ mechanism") as that responsible for the dynamic spectral behavior of the great majority of these compounds in the presence of added basic ligands.[3,4] However, the mechanisms represented by eq 2 and 3 have also been invoked in discussions of dynamic spectral behavior of *trihapto*allyl compounds, not only in the presence of added bases but also in the *absence* of added donor ligands, although without convincing experimental basis.[5-9] The problem of identifying the mechanism responsible for dynamic behavior in solutions containing added bases is clearly one which cannot be solved using the techniques employed in their absence,[2-4,7] since the addition of donor ligands to a solution containing a *trihapto*allyl organometallic reagent could in principle lead to a change in mechanism from that represented by eq 3 to that of eq 1 or 2. However, the mechanism of eq 3, hereafter referred to as the "concerted mechanism," differs fundamentally from that represented by eq 1 or 2, in that the interchange of both pairs of syn and anti protons at the termini of the allyl moiety occurs simultaneously in the former, while the interchange of syn and anti protons in the latter is restricted to one terminus at a time. The extent to which the motion resulting in proton interchange at one end of the allyl group is correlated (or anticorrelated) with that at the other end thus provides a possible basis for distinguishing between these two classes of mechanisms.[10]

In this paper we report the results of a reexamination of the dynamic nmr spectrum of tetra(*trihapto*allyl)zirconium-(IV) (**5**) in fluorotrichloromethane, first discussed by Becconsall, Job, and O'Brien,[7] and a full interpretation of the dynamic line shapes observed for this compound in terms of

(1) This work was supported by the National Institutes of Health (Grant HL 15029), the donors of the Petroleum Research Fund, administered by the American Chemical Society (Grant 4032), and the National Science Foundation (Grant GP 31930).

(2) National Institutes of Health Predoctoral Fellow, 1967–1968.

(3) For recent reviews, see J. W. Faller, M. E. Thomsen, and M. J. Mattina, *J. Amer. Chem. Soc.*, **93**, 2642 (1971); L. A. Fedorov, *Russ. Chem. Rev.*, **39**, 655 (1970); P. M. Maitlis, "The Organic Chemistry of Palladium," Vol. I, Academic Press, New York, N. Y., 1971; K. Vrieze and P. W. N. M. van Leeuwen, *Progr. Inorg. Chem.*, **14**, 1 (1971).

(4) For examples, see K. Vrieze, A. P. Praat, and P. Cosee, *J. Organometal. Chem.*, **12**, 533 (1965); F. A. Cotton, J. W. Faller, and A. Musco, *Inorg. Chem.*, **6**, 179 (1967); J. W. Faller, M. J. Incorvia, and M. E. Thomsen, *J. Amer. Chem. Soc.*, **91**, 518 (1969); J. W. Faller and M. E. Thomsen, *ibid.*, **91**, 6871 (1969); D. L. Tibbetts and T. L. Brown, *ibid.*, **92**, 3031 (1970); and references in each.

(5) *Cf.* the remarks of F. A. Cotton in the discussion following the article by G. Wilke, *Proc. Robert A. Welch Found. Conf. Chem. Res.*, **9**, 184 (1965).

(6) F. De Candia, G. Maglio, A. Musco, and G. Paiaro, *Inorg. Chim. Acta*, **2**, 233 (1968).

(7) J. K. Becconsall, B. E. Job, and S. O'Brien, *J. Chem. Soc. A*, 423 (1967).

(8) G. Wilke, *et al.*, *Angew. Chem., Int. Ed. Engl.*, **5**, 151 (1966).

(9) K. C. Ramey, D. C. Lini, and W. B. Wise, *J. Amer. Chem. Soc.*, **90**, 4275 (1968).

the extent of correlation of the proton-interchange processes occurring at the ends of its allyl groups. This work illustrates a technique that can be used quite generally to distinguish between the two types of mechanisms represented by eq 3 and by eq 1 and 2 that does not rely on inferring the behavior of the organometallic compound in the *absence* of added ligands from its behavior in their presence. In addition, it provides an opportunity to compare the results of approximate and "complete" calculations of interchange-broadened line shapes and to establish the extent to which small spin-spin coupling constants may determine mechanistically important details of these line shapes in tightly coupled spin systems.

## Results

The $^1$H nmr spectrum of 5 in fluorotrichloromethane changes from a typical $AX_4$ pattern at the fast-exchange limit ($-20°$) to an $AM_2X_2$ spectrum at $-80°$ ($\delta_A$ 5.24, $\delta_M$ 3.32, $\delta_X$ 1.90).[11,12] The downfield portion of the slow-exchange spectrum of 5 is characterized by a triplet of triplets



$$(4)$$

5
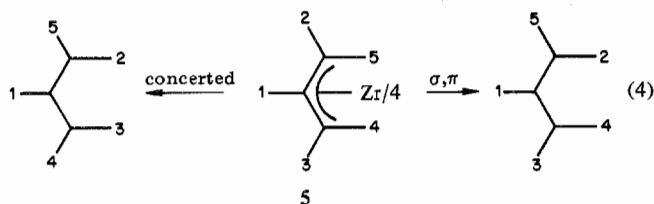
with $J_{12} = J_{13} = 9.2$ Hz and $J_{14} = J_{15} = 16.0$ Hz. There is no direct evidence in the slow-exchange spectrum of four-bond couplings exceeding *ca.* 2.0 Hz in magnitude between the protons of the methylene groups. Nonetheless, the widths of the lines are such that small couplings would not be observed directly, and indirect evidence cited below indicates that these couplings are important in determining line shapes

(10) In principle, additional fine distinctions could be drawn in postulating mechanisms resulting in the same permutational result as that characterizing either the $\sigma,\pi$ or concerted mechanisms (eq 3). Thus, for example, a variety of reactions could be imagined that transfer allylic hydrogen from one carbon to another. We exclude all such mechanisms as physically unreasonable. Further, within the classes of reaction which leave C–H bonds intact, it is *a priori* possible that a process resulting in simultaneous interchange of both sets of terminal methylene protons might take place by the motion described in eq 3, in which the direction of rotation of both methylene groups is the same (i), or by another type of motion (ii), in which the methylene



i             ii
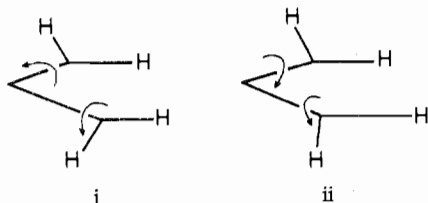
groups rotate in opposite senses. We believe the type of mechanism represented by ii to be unreasonable in the particular system under study. More generally, the distinction of two permutationally identical processes differing only in the "mode" of the process is discussed at length in other connections [J. I. Musher, *J. Amer. Chem. Soc.*, **94**, 5662 (1972)] is not presently a useful one in dynamic nmr spectroscopy, since no techniques are available for their experimental investigation. The two permutational schemes discussed here are the only intramolecular schemes that leave C–H bonds intact.

(11) At $-80°$ the four *trihapto*allyl groups of 5 are magnetically equivalent, either as a result of geometrical equivalence or as a result of rotation around the metal–allyl bond.[12] Below $-90°$ there is evidence of further broadening of the downfield multiplet and upfield doublets, accompanied by formation of an additional multiplet at $\delta \sim 3.5$–4.0. This spectral change may be due to isolation of a geometric isomer. Poor spectral resolution does not permit further conjecture.

(12) Related effects have been observed in the spectra of tri-(*trihapto*allyl)rhodium(III): J. K. Becconsall and S. O'Brien, *Chem. Commun.*, 720 (1966).

in the region of intermediate exchange rates.

**Procedure for Spectral Simulation.** Spectra were calculated for the $H_1$ resonance of 5 using the density matrix technique of Kaplan and Alexander.[13] This approach is based on solution of the phenomenological equation of motion of the density matrix $\rho$[13] (eq 5). Here $\mathcal{H} = \mathcal{H}_0 + \mathcal{H}_1$ is the usual

$$\frac{\partial \rho}{\partial t} = i[\rho, \mathcal{H}] - \rho/T_2 + \left(\frac{\partial \rho}{\partial t}\right)_{\text{exchange}} \tag{5}$$

Hamiltonian describing the interaction of the nuclear spins with the external magnetic field, with the driving radiofrequency field, and with one another through spin–spin couplings; $\rho/T_2$ describes relaxation effects in the absence of the proton interchange reactions of interest; and the last term defines the influence of this interchange on $\rho$.[14]

When $\rho$ is expressed using the eigenfunctions $\psi$ of $\mathcal{H}_0$ as basis functions, eq 5 assumes a form that is particularly easily interpreted physically. Calling the nuclear spin product functions $\phi$, these eigenfunctions can be expressed in matrix form by eq 6. The influence of a process resulting in mutual inter-

$$\psi = H\phi \tag{6}$$

change of protons on the product functions $\phi$ can be described by an equation of the form of eq 7, following the permuta-

$$\phi_{\text{after} \atop \text{interchange}} = X^q \phi_{\text{before} \atop \text{interchange}} \tag{7}$$

tion procedure originally introduced by Kaplan and Alexander.[13] The superscript q of the matrix $X^q$ is an index used to label a particular interchange process in instances in which several are possible. The corresponding change imposed by the proton interchange on the eigenfunctions is given by eq 8 and reflected in $\rho$ for cases involving mutual

$$\psi_{\text{after} \atop \text{interchange}} = R^q \psi_{\text{before} \atop \text{interchange}} = H \cdot X^q \cdot H^{-1} \psi_{\text{before} \atop \text{interchange}} \tag{8}$$

exchange, again using procedures outlined by Alexander,[13] by four equivalent expressions (eq 9). In these equations, $1/\tau_q$ is the pseudo-first-order rate constant for the qth interchange process, and the matrix of coefficients in eq 9d is named the kinetic exchange matrix $K$.[15]

$$\left(\frac{\partial \rho}{\partial t}\right)_{\text{interchange}} = \frac{\rho_{\text{after} \atop \text{interchange}} - \rho_{\text{before} \atop \text{interchange}}}{\tau_q} \tag{9a}$$

$$\left(\frac{\partial \rho}{\partial t}\right)_{\text{interchange}} = \frac{R^q \rho_{\text{before} \atop \text{interchange}} R^q - \rho_{\text{before} \atop \text{interchange}}}{\tau_q} \tag{9b}$$

$$\left(\frac{\partial \rho_{kl}}{\partial t}\right)_{\text{interchange}} = \frac{\sum_{q} \sum_{i,j} R^q_{ki} \rho_{ij} R^q_{jl} - \rho_{kl}}{\tau_q} \tag{9c}$$

$$\left(\frac{\partial \rho}{\partial t}\right)_{\text{interchange}} = K\rho \tag{9d}$$

(13) J. I. Kaplan, *J. Chem. Phys.*, **28**, 278 (1958); **29**, 462 (1958); S. Alexander, *ibid.*, **37**, 967, 974 (1962); **38**, 1787 (1963); **40**, 2741 (1964).

(14) The application of eq 5 to problems of chemical exchange in nmr spectroscopy has been extensively reviewed: (a) C. S. Johnson, *Advan. Magn. Resonance*, **1**, 33 (1965); (b) G. Binsch, *Top. Stereochem.*, **3**, 97 (1968); (c) R. M. Lynden-Bell, *Progr. Nucl. Magn. Resonance Spectrosc.*, **2**, 163 (1967); I. O. Sutherland, *Annu. Rev. NMR Spectrosc.*, **4**, (1971). See also P. D. Sullivan and J. R. Bolton, *Advan. Magn. Resonance*, **4**, 39 (1970), and P. W. Watkins, *Mol. Phys.*, **13**, 37 (1967), for related applications to epr spectroscopy.

(15) For further details of the background and development of these equations, consult the Ph.D. thesis of J. K. Krieger, Massachusetts Institute of Technology, Cambridge, Mass., 1971.

In the representation of eigenfunctions of the Hamiltonian, the off-diagonal elements of $\rho$ are directly connected to transitions in the observable spectrum. Since only resonances with nonzero intensities need be considered in analyzing the line shapes of exchange-broadened spectra and since in consequence only elements of the density matrix corresponding to observed transitions are coupled in the series of linear equations generated by the combination of eq 5 and 9, it is sufficient to limit consideration to these elements of $\rho$ in obtaining an analytical expression for the line shape. Thus, assuming that only one type of interchange process is important in determining line shapes (that is, that two or more nuclear permutational schemes are not required to characterize the reaction) the index q in eq 9c can be dropped; further, using a single subscript n to refer to the density matrix element between the eigenfunction $\psi_k$ and $\psi_l$, eq 9c can be rewritten as eq 9e. The element $\rho_n$ now describes a

$$\left(\frac{\partial \rho_n}{\partial t}\right)_{\text{interchange}} = \frac{\sum_m \mathbf{K}_{nm}\rho_m}{\tau} \tag{9e}$$

$$\rho_n \equiv \rho_{kl}$$

single transition in the observed spectrum, and the matrix elements $\mathbf{K}_{nm}$ can be considered physically to be rate constants describing the transfer of magnetization from the transition $n$ to transition $m$ as a result of the nuclear interchange.

Using this particular simple form for the exchange term in eq 5 and evaluating terms due to $\mathcal{H}$ in the resulting combined equation with application of the usual high-temperature approximation,[13] a final line shape equation describing the absorption intensity of the spectrum as a function of the frequency $\omega$ (in radians per second) can be expressed (eq 10) in the same form as the equation derived by Sack[16] for molecules lacking spin-spin coupling. Here $\mathbf{I} = (I_1, I_2 \cdots, I_n)$ is a

$$I(\omega) \propto \text{Re}[\mathbf{I} \cdot \mathbf{A}^{-1} \cdot \mathbf{1}] \tag{10}$$

row vector containing the intensities ($I_n$) of the observed lines, $\mathbf{1}$ is a unit column vector, and $\mathbf{A}$ is given by eq 11,

$$\mathbf{A} = \begin{pmatrix} -\alpha_1 + K_{11}/\tau & K_{12}/\tau & K_{13}/\tau & \cdot & \cdot \\ K_{21}/\tau & -\alpha_2 + K_{22}/\tau & K_{23}/\tau & \cdot & \cdot \\ K_{31}/\tau & K_{32}/\tau & -\alpha_3 + K_{33}/\tau & \cdot & \cdot \\ \cdot & \cdot & \cdot & \cdot & \cdot \\ \cdot & \cdot & \cdot & \cdot & \cdot \end{pmatrix} \tag{11}$$

where $\alpha_n = 2\pi i(\omega_n - \omega) + (1/T_2)_n$, the $\omega_n$ are the frequencies of the observed lines, and the elements $\mathbf{K}_{nm}$ are the elements of the kinetic exchange matrix. Equation 10 is conveniently solved using numerical methods based on the separation of $\mathbf{A}$ into frequency-independent and -dependent parts, diagonalization of the former, and the use of a diagonalizing transformation to effect the efficient inversion of $\mathbf{A}$.[17,18]

This entire procedure is functionally equivalent to that used by Binsch[17] and widely applied elsewhere, differing conceptually only to the extent of a similarity transformation required to transform from the basis of nuclear spin product functions to the basis of eigenfunctions of the spin Hamiltonian. It suffers in practice from being slightly more cumbersome than Binsch's procedure but has the compensating advantage that the elements of the $\mathbf{K}$ matrix, in

combination with the intensities of the lines, can be used to give a physically transparent interpretation of the manner in which magnetization is transferred between lines by the interchange process. It resembles closely the procedure used in the examination of $H_2Fe[P(OC_2H_5)_3]_4$ by Meakin, Muetterties, Tebbe, and Jesson.[19]

**Calculated Spectra. Approximate Calculations Based on Symmetrized Nuclear Spin Wave Functions.** Spectra were calculated for proton $H_1$ of **5** at three levels of complexity: first, the spin system of the allyl moieties was approximated as an $AX_2Y_2$ system, having only $J_{AX}$ and $J_{AY}$ nonzero; second, the spectrum was simulated as an $AM_2N_2$ system, using correct chemical shifts, but still assuming nonzero values only for $J_{AM}$ and $J_{AN}$; and, third, a "complete" calculation was carried through, taking into account the effects of the small two- and four-bond spin-spin couplings, $J_{23}$ and $J_{25}$. Although only the last of these calculations gave spectra that could be used as the basis for a reliable mechanistic distinction between the $\sigma,\pi$ and concerted classes of mechanisms for the proton-interchange reactions, the results of the simpler calculations are also summarized here for two reasons. First, these calculations permit a clearer physical interpretation of the dynamic behavior of the spectrum of **5** than do the more complex "complete" calculations; and, second, a comparison of the spectra obtained at these three levels of completeness, both with one another and with the experimental spectra, provides a practical illustration of the influence of relatively small coupling constants on the line shapes of tightly coupled dynamic spin systems.

In the simplest analysis, the resonances observed for $H_1$ can be interpreted in terms of transitions between easily visualized spin configurations (Figure 1). Thus, the transition occurring at lowest frequency, labeled 1 in this diagram, is due to the flip of $H_1$ from a $\beta$ to an $\alpha$ orientation with respect to the external field, in the magnetic environment provided by the four other protons in the molecule, $H_2$, $H_3$, $H_4$, and $H_5$, each in $\alpha$ orientations (eq 12). Similarly, at this level of analysis, each of the other transitions can be assigned to the flip of $H_1$ from a $\beta$ to an $\alpha$ state in the presence of some well-defined

$$\beta_1[\alpha_2\alpha_3\alpha_4\alpha_5] \rightarrow \alpha_1[\alpha_2\alpha_3\alpha_4\alpha_5] \tag{12}$$

$$\beta_1\chi_j \rightarrow \alpha_1\chi_j \tag{13}$$
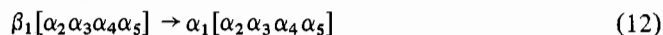
configuration of spins for the four protons $H_2$, $H_3$, $H_4$, and $H_5$. Since we are assuming at this juncture that the spectrum is first order, each of these transitions can be written as indicated in eq 13, where the function $\chi_j$ represents the spin configuration of $H_{2-5}$. In a full treatment, these functions would be the eigenfunctions of the time-independent nuclear spin Hamiltonian; as a first approximation, we take these $\chi_j$ to be simply the symmetrized wave functions for four protons in $C_2$ nuclear symmetry (Figure 1).[20] Each of the observed transitions is labeled by the appropriate $\chi_j$ and, for later reference, by the symmetry of each of these $\chi_j$.

Thus, at the simplest level of interpretation, the observed spectrum of $H_1$ can be thought of as due to the $H_1$ resonances in a mixture of 16 distinct types of $\pi$-allyl moieties (each differing from the others in the arrangement of the spins of $H_2$, $H_3$, $H_4$, and $H_5$ with respect to the external field and to each other). The problem of interpreting the temperature dependence of this system of resonances in terms of $\sigma,\pi$ or concerted mechanisms then becomes that of

(16) R. A. Sack, *Mol. Phys.*, **1**, 163 (1958).

(17) G. Binsch, *J. Amer. Chem. Soc.*, **91**, 1304 (1969).

(18) R. G. Gordon and R. P. McGinnis, *J. Chem. Phys.*, **49**, 2455 (1968); R. E. Schirmer, J. H. Noggle, and D. F. Gaines, *J. Amer. Chem. Soc.*, **91**, 6240 (1969).

(19) P. Meakin, E. L. Muetterties, F. N. Tebbe, and J. P. Jesson, *J. Amer. Chem. Soc.*, **93**, 4701 (1971).

(20) J. W. Emsley, J. Feeney, and L. H. Sutcliffe, "High Resolution Nuclear Magnetic Resonance Spectroscopy," Vol. I, Pergamon Press, Oxford, 1965, Chapter 8.
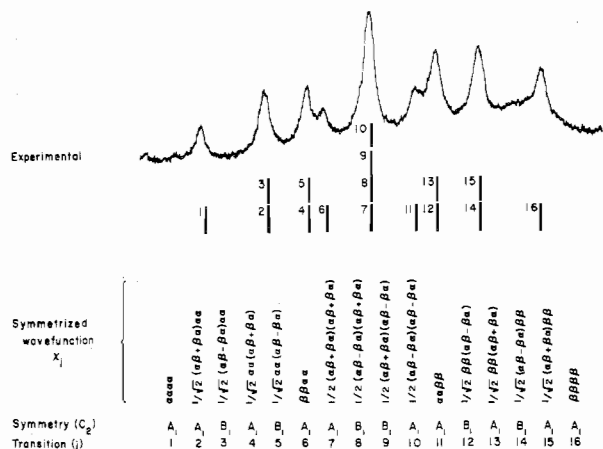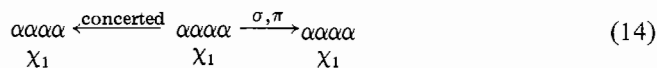
**Figure 1.** Symmetrized wave functions in $C_2$ symmetry and spectral assignments for the H$_1$ portion of the spectrum of tetra(*trihapto*-allyl)zirconium(IV) (5).

understanding how these allyl moieties are interconverted by the two distinct types of mechanisms. These interconversion schemes are of course readily worked out in any general case by the formalism described in eq 6-11; however, at this level of approximation, they can also be derived readily using simple physical arguments, and these agruments are sketched here.

In nmr spectra of the type considered in this work, spectral lines broaden and coalesce as a result of a dynamic process only when the precession frequency of the proton(s) whose resonance is being observed is changed by the process. Thus, for example, the rate of chemical exchange of protons between water molecules in a sample of pure water has no influence on the shape of the water proton signal, since all of the sites connected by the exchange have indistinguishable chemical shifts; however, the rate of chemical exchange of protons in a sample containing water and hydrogen peroxide determines whether distinct $H_2O$ and $H_2O_2$ resonances, a single averaged signal, or a broadened intermediate resonance is observed, since the precession frequencies of protons on water and hydrogen peroxide are distinguishable. The transition labeled 1 in the spectrum of tetra(*trihapto*allyl)zirconium is the resonance of proton 1 in the characteristic magnetic environment provided by $H_{2-5}$ in $\alpha$-spin states. Clearly, no permutation of these latter protons, whether by $\sigma,\pi$ or by concerted mechanisms, will change the environment experienced by $H_1$ (eq 14). Thus, transition 1 will be unaffected by either $\sigma,\pi$ or concerted reactions.

$$\underset{\chi_1}{\alpha\alpha\alpha\alpha} \xleftarrow{\text{concerted}} \underset{\chi_1}{\alpha\alpha\alpha\alpha} \xrightarrow{\sigma,\pi} \underset{\chi_1}{\alpha\alpha\alpha\alpha} \qquad (14)$$

To rationalize the behavior of the transition labeled 2 in Figure 1 (the $1/\sqrt{2}\beta(\alpha\beta + \beta\alpha)\alpha\alpha \rightarrow 1/\sqrt{2}\alpha(\alpha\beta + \beta\alpha)\alpha\alpha$ transition) under the two types of interchange mechanisms in physical terms, it is helpful to think in terms of an essentially classical description of the motion of the nuclear magnetic dipole moment of $H_1$ in the characteristic magnetic field provided by the spin configuration $\chi_2$. In a description of this type, the precession at frequency $\omega_i$ of a particular proton $H_i$ in an $\alpha$-spin state in a local magnetic field $H_i$ is represented by the motion of a vector $\mu_i$ around the surface of a cone having the effective magnetic field vector $H_1$ as its principal axis (Figure 2).[21] The field $H_1$ is assumed to be the

(21) For elaboration of the background and limitations of this approach, see W. Kauzmann, "Quantum Chemistry," Academic Press, New York, N. Y., 1957, pp 305-315.
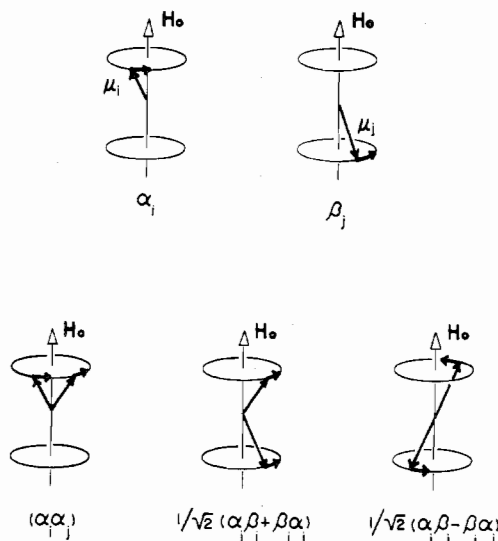


**Figure 2.** Classical representation of the precession of protons in a magnetic field.

only field experienced by $\mu_i$ and includes the contributions of the external magnetic field $H_0$, the modification of this field due to electronic screening (described by the chemical shift term), and further modifications due to indirect interactions with other magnetic nuclei (described by the spin-spin coupling constants).[22] A $\beta$-spin state is represented in an analogous manner (Figure 2). Any reaction that produces dynamic line-broadening effects in a transition of $H_i$ occurring at frequency $\omega_i$ will do so by changing $H_i$, and consequently $\omega_i$. Conversely, a process that does *not* change $\omega_i$ (such as the permutation of protons in $\chi_1$ discussed above) will not affect this transition. Sets of two magnetically equivalent nuclei can also be represented within the same classical picture. Thus, many of the properties of a $1/\sqrt{2}(\alpha_i\beta_j + \beta_i\alpha_j)$ spin state can be derived from consideration of two magnetic moment vectors, one $\alpha$ and one $\beta$, precessing *in phase* at the same angular frequency; a $1/\sqrt{2}(\alpha_i\beta_j - \beta_i\alpha_j)$ state can be similarly represented by two vectors precessing 180° out of phase.[21]

Within this classical picture, it is straightforward to rationalize the influence of concerted and $\sigma,\pi$ proton-interchange reactions on the spin state $\chi_2$ and on the transition labeled 2 in Figure 1. We describe the $1/\sqrt{2}(\alpha_2\beta_3 + \beta_2\alpha_3)\alpha_4\alpha_5$ configuration of spins by a diagram which constitutes an obvious extension of those already discussed (Figure 3): $1/\sqrt{2}(\alpha_2\beta_3 + \beta_2\alpha_3)$ is represented by two spins, one $\alpha$ and one $\beta$, precessing in phase under the influence of a local field $H_x$ at frequency $\omega_x$, and $\alpha_4\alpha_5$ is represented by two $\alpha$ spins precessing under the influence of a local field $H_y$ at frequency $\omega_y$. The concerted interchange reaction has the effect of switching $H_x$ and $H_y$; that is, the two pairs of spins simply interchange precession frequencies without altering phase relations within the pairs. Thus, the concerted interchange reaction has the effect of converting the spin configuration $\chi_2$ into $\chi_4$. Describing the influence of the $\sigma,\pi$ interchange on $\chi_2$ is more

(22) Spin-spin coupling terms can be included in this manner only in a first-order spectrum, that is, in circumstances in which the precession frequency $\omega_i$ of proton $H_i$ differs sufficiently from that of any of the other protons to which it is coupled that spin-spin contributions to the magnetic field at $\mu_i$ along the directions perpendicular to the external magnetic field $H_0$ are felt only as fluctuations occurring at a frequency too high for the precessional motion of $\mu_i$ to respond significantly. Under these circumstances, the only detectable contributions to $\omega_i$ from other spins are those resulting from magnetic interactions having components parallel to the direction of the external magnetic field.
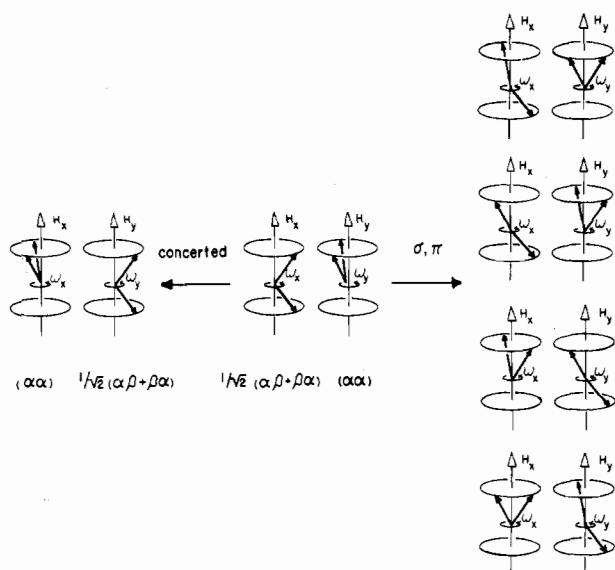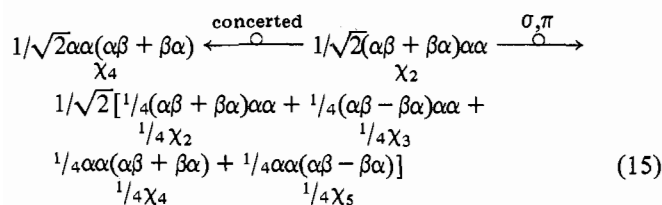
**Figure 3.** Classical description of the influence of $\sigma,\pi$ and concerted interchange events on the proton spin configuration $\chi_2 = 1/\sqrt{2}(\alpha\beta + \beta\alpha)\alpha\alpha$.

**Table I.** Spin Configurations for the Allyl Groups of 1 before and after Proton Interchange by Concerted and $\sigma,\pi$ Mechanisms[a]

| Concerted | | $\sigma,\pi$ |
|---|---|---|
| $(\chi_j)_{\text{after}}$ | $(\chi_j)_{\text{before}}$ | $(\chi_j)_{\text{after}}$ |
| $\chi_1 \longleftarrow$ | $\chi_1$ | $\longrightarrow \chi_1$ |
| $\chi_4 \longleftarrow$ | $\chi_2$ | $\longrightarrow 1/4[\chi_2 + \chi_3 + \chi_4 + \chi_5]$ |
| $\chi_5 \longleftarrow$ | $\chi_3$ | $\longrightarrow 1/4[\chi_2 + \chi_3 + \chi_4 + \chi_5]$ |
| $\chi_2 \longleftarrow$ | $\chi_4$ | $\longrightarrow 1/4[\chi_2 + \chi_3 + \chi_4 + \chi_5]$ |
| $\chi_3 \longleftarrow$ | $\chi_5$ | $\longrightarrow 1/4[\chi_2 + \chi_3 + \chi_4 + \chi_5]$ |
| $\chi_{11} \longleftarrow$ | $\chi_6$ | $\longrightarrow 1/4[\chi_7 + \chi_8 + \chi_9 + \chi_{10}]$ |
| $\chi_{10} \longleftarrow$ | $\chi_7$ | $\longrightarrow 1/4[\chi_6 + \chi_7 + \chi_{10} + \chi_{11}]$ |
| $\chi_9 \longleftarrow$ | $\chi_8$ | $\longrightarrow 1/4[\chi_6 + \chi_8 + \chi_9 + \chi_{11}]$ |
| $\chi_8 \longleftarrow$ | $\chi_9$ | $\longrightarrow 1/4[\chi_6 + \chi_8 + \chi_9 + \chi_{11}]$ |
| $\chi_7 \longleftarrow$ | $\chi_{10}$ | $\longrightarrow 1/4[\chi_6 + \chi_7 + \chi_{10} + \chi_{11}]$ |
| $\chi_6 \longleftarrow$ | $\chi_{11}$ | $\longrightarrow 1/4[\chi_7 + \chi_8 + \chi_9 + \chi_{10}]$ |
| $\chi_{14} \longleftarrow$ | $\chi_{12}$ | $\longrightarrow 1/4[\chi_{12} + \chi_{13} + \chi_{14} + \chi_{15}]$ |
| $\chi_{15} \longleftarrow$ | $\chi_{13}$ | $\longrightarrow 1/4[\chi_{12} + \chi_{13} + \chi_{14} + \chi_{15}]$ |
| $\chi_{12} \longleftarrow$ | $\chi_{14}$ | $\longrightarrow 1/4[\chi_{12} + \chi_{13} + \chi_{14} + \chi_{15}]$ |
| $\chi_{13} \longleftarrow$ | $\chi_{15}$ | $\longrightarrow 1/4[\chi_{12} + \chi_{13} + \chi_{14} + \chi_{15}]$ |
| $\chi_{16} \longleftarrow$ | $\chi_{16}$ | $\longrightarrow \chi_{16}$ |

[a] The entries in this table should be interpreted to mean, *e.g.*, that an allyl moiety originally described by a nuclear spin wave function $\chi_2$ (as expanded in Figure 1) *before* proton interchange by the $\sigma,\pi$ mechanism would be found in states described by $\chi_2$, $\chi_3$, $\chi_4$, and $\chi_5$ with equal probability *after* the interchange.

complicated. As a result of an interchange event of this type, one of the two protons precessing at $\omega_x$ exchanges with one of the two precessing at $\omega_y$; the four classically distinct spin configurations resulting from this exchange are indicated schematically in the figure. Since there is no relation between the phases of the pairs of protons precessing at $\omega_x$ and $\omega_y$ *before* the exchange, the phase within the pairs *after* the exchange is arbitrary. Two $\alpha$ spins precessing at the same frequency are described by the spin function $\alpha\alpha$, regardless of phase; the pairs of $\alpha$ and $\beta$ spins precessing with the same frequency are equally likely to have a 0 or 180° phase angle between them and are thus described with equal probability by $1/\sqrt{2}(\alpha\beta + \beta\alpha)$ spin functions. Thus, the influence of the concerted and $\sigma,\pi$ interchanges on $\phi_2$ is summarized in eq 15 which states, for example, that the spin configuration represented by $\chi_2$ before interchange is converted to the spin configuration represented by $\chi_4$ by the concerted mechanism; that is, $(\chi_2)_{\text{after interchange}} = (\chi_4)_{\text{before interchange}}$. Analogous arguments apply to $\chi_3$, $\chi_4$, and $\chi_5$; the results of these arguments are summarized in Table I.

$$1/\sqrt{2}\alpha\alpha(\alpha\beta + \beta\alpha) \xleftarrow{\text{concerted}} 1/\sqrt{2}(\alpha\beta + \beta\alpha)\alpha\alpha \xrightarrow{\sigma,\pi}$$
$$\chi_4 \qquad\qquad \chi_2$$
$$1/\sqrt{2}[1/4(\alpha\beta + \beta\alpha)\alpha\alpha + 1/4(\alpha\beta - \beta\alpha)\alpha\alpha +$$
$$1/4\chi_2 \qquad\qquad 1/4\chi_3$$
$$1/4\alpha\alpha(\alpha\beta + \beta\alpha) + 1/4\alpha\alpha(\alpha\beta - \beta\alpha)] \qquad (15)$$
$$1/4\chi_4 \qquad\qquad 1/4\chi_5$$

These same conclusions concerning the influence of the two possible mechanisms for interchange on the spin functions $\chi_i$ can be reached directly and simply by manipulation of these spin functions following the procedure outlined by Kaplan. The concerted process interchanges proton 2 with proton 5, and proton 3 with proton 4 (eq 16), while the $\sigma,\pi$ process interchanges one pair (either proton 3 with proton 4,
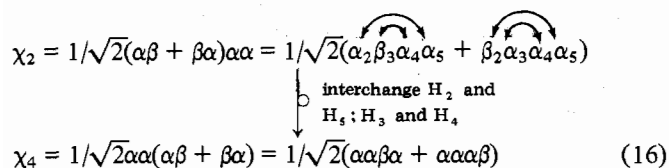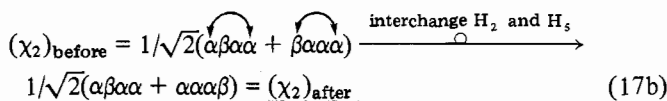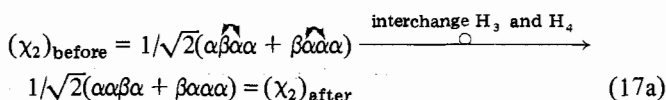
$$\chi_2 = 1/\sqrt{2}(\alpha\beta + \beta\alpha)\alpha\alpha = 1/\sqrt{2}(\alpha_2\beta_3\alpha_4\alpha_5 + \beta_2\alpha_3\alpha_4\alpha_5)$$

interchange $H_2$ and $H_5$; $H_3$ and $H_4$

$$\chi_4 = 1/\sqrt{2}\alpha\alpha(\alpha\beta + \beta\alpha) = 1/\sqrt{2}(\alpha\alpha\beta\alpha + \alpha\alpha\alpha\beta) \qquad (16)$$

eq 17a, or proton 2 with proton 5, eq 17b). To express the

$$(\chi_2)_{\text{before}} = 1/\sqrt{2}(\alpha\beta\alpha\alpha + \beta\alpha\alpha\alpha) \xrightarrow{\text{interchange } H_3 \text{ and } H_4}$$
$$1/\sqrt{2}(\alpha\alpha\beta\alpha + \beta\alpha\alpha\alpha) = (\chi_2)_{\text{after}} \qquad (17a)$$

$$(\chi_2)_{\text{before}} = 1/\sqrt{2}(\alpha\beta\alpha\alpha + \beta\alpha\alpha\alpha) \xrightarrow{\text{interchange } H_2 \text{ and } H_5}$$
$$1/\sqrt{2}(\alpha\beta\alpha\alpha + \alpha\alpha\alpha\beta) = (\chi_2)_{\text{after}} \qquad (17b)$$

spin functions resulting from these two equally probable $\sigma,\pi$ interchanges in terms of the symmetrized functions used as a basis set (Figure 1), we take advantage of the simple relations in eq 18. Thus, substituting eq 18 into 17a one obtains eq 19a, and similarly eq 19b from eq 17b. Equations 16 and 19

$$\alpha\beta = 1/2[(\alpha\beta + \beta\alpha) + (\alpha\beta - \beta\alpha)] \qquad (18a)$$

$$\beta\alpha = 1/2[(\alpha\beta + \beta\alpha) - (\alpha\beta - \beta\alpha)] \qquad (18b)$$

$$(\chi_2)_{\text{after}} = 1/\sqrt{2}(\alpha\beta\alpha\alpha + \alpha\alpha\alpha\beta) = 1/2(\chi_2 - \chi_3 + \chi_4 - \chi_5) \qquad (19a)$$

$$(\chi_2)_{\text{after}} = 1/\sqrt{2}(\alpha\alpha\beta\alpha + \beta\alpha\alpha\alpha) = 1/2(\chi_2 + \chi_3 + \chi_4 + \chi_5) \qquad (19b)$$

express the nuclear spin wave functions after exchange as a linear combination of those before exchange. In order to obtain from these equations the probabilities, listed in Table I, that a molecule originally described by $\chi_2$ will appear as $\chi_2$, $\chi_3$, $\chi_4$, or $\chi_5$ after the interchange event, the coefficients of these equations are simply squared in the usual manner; in addition, since 3,4 and 2,5 interchanges are equally probable in the $\sigma,\pi$ mechanism, these squared coefficients are averaged for each $\chi_j$.

Both of these manipulations and the classical physical arguments outlined above lead to the same conclusions concerning the behavior of transitions 2–5 in the intermediate exchange rate; *viz.*, in both the $\sigma,\pi$ and concerted mechanisms, magnetization from the degenerate 2,3 transitions will exchange with magnetization from the degenerate 4,5 transitions, and the two distinguishable spectral lines observed at the slow exchange limit will broaden and coalesce with one another, but not with other lines in the spectrum, on increasing the proton interchange rates.

Although the behavior of these lines is qualitatively similar, the probabilities given in Table I indicate that the response of the line shapes to interchange rate do differ quantitatively in the two mechanisms. In the $\sigma,\pi$ mechanism, magnetization originating in transition 2 either remains in this transition or transfers to transition 3 in half of the interchange events, and these events then contribute nothing to line broadening since no change in the resonance frequency of $H_1$ is involved; in the concerted mechanism, each interchange event results in transfer of magnetization between magnetically distinct sites and thus leads to broadening. Nevertheless, the fact that coalescence of the 2,3 and 4,5 lines will occur for a rate of concerted interchange half that required for coalescence under the $\sigma,\pi$ interchange is useless, since there is no independent way of measuring these rates. Thus, the behavior of the 2,3 and 4,5 lines (and by analogous arguments, the 12,13 and 14,15 lines) cannot be employed in distinguishing between the concerted and $\sigma,\pi$ mechanisms.

Similar lines of reasoning provide the basis for understanding the behavior of transitions 6-11 in the region of exchange-broadened line shapes. However, an interesting difference in the exchange schemes predicted by the classical physical argument and that obtained by manipulation of the symmetrized wave functions points up the limitations of the former. In applying these classical arguments first to transition 6, the transition of $H_1$ in the magnetic environment provided by $H_{2-5}$ in a $\beta\beta\alpha\alpha$ configuration, it is helpful to construct a diagram (Figure 4) analogous to Figure 3. Clearly the concerted process will simply interchange the sites and precession frequencies of the two $\alpha$ and $\beta$ nuclei. A $\sigma,\pi$ mechanism will interchange one $\alpha$ with one $\beta$ proton. Since the classical phase angle between the resulting pairs of $\alpha$ and $\beta$ nuclei precessing at the same frequency will assume every value between 0 and $2\pi$, the probabilities of generating $\chi_7$, $\chi_8$, $\chi_9$, and $\chi_{10}$ from $\beta\beta\alpha\alpha$ (or from $\alpha\alpha\beta\beta = \chi_{11}$) are equal. Permutation of the nuclei using the Kaplan procedure yields an identical conclusion.

These two procedures do, however, apparently yield different predictions when applied to any one of the transitions 7-10. Figure 5 is an appropriate classical diagram for $\chi_7 = {}^1/_2(\alpha\beta + \beta\alpha)(\alpha\beta + \beta\alpha)$. A concerted interchange converts $\chi_7$ into $\chi_7$; that is, before and after the interchange event protons $H_{2-5}$ are in spin configurations that are identical, with the possible exception of classical phase shifts that are undetectable in their influence on the magnetic field experienced at $H_1$ through spin–spin coupling. The $\sigma,\pi$ mechanism clearly converts $\chi_7$ to $\alpha\alpha\beta\beta$ and $\beta\beta\alpha\alpha$ with normalized probabilities of 0.25 each and with a probability of 0.5 to spin configurations having paired $\alpha$ and $\beta$ nuclei. Since the classical phase angle between the members of these pairs can assume any value with equal probability, it would appear that the spin configurations $\chi_7$, $\chi_8$, $\chi_9$, and $\chi_{10}$ would have equal probabilities of being created from $\chi_7$ by this mechanism. Nevertheless, application of the Kaplan procedure leads to the more restricted conclusion that $\chi_7$ is converted with equal probabilities only to $\chi_6$, $\chi_7$, $\chi_{10}$, and $\chi_{11}$ by the $\sigma,\pi$ mechanism (eq 20). In this equation, only interchange of $H_2$ and $H_5$ is considered; the same conclusion is reached
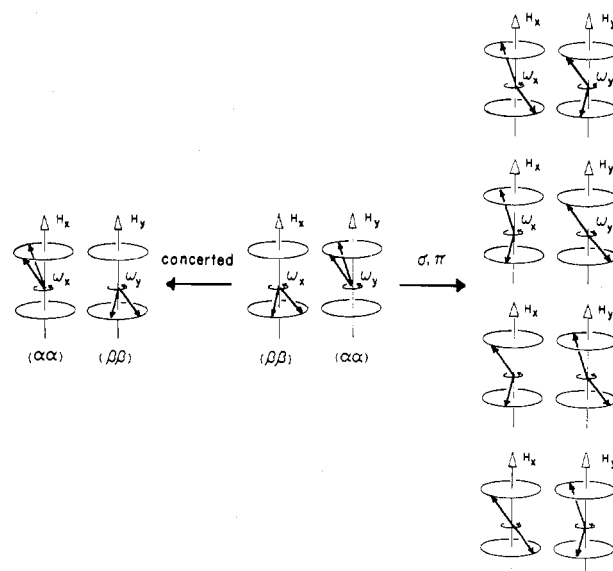


**Figure 4.** Classical representation of the influence of $\sigma,\pi$ and concerted interchange events on the proton spin configuration $\chi_6 = \beta\beta\alpha\alpha$.
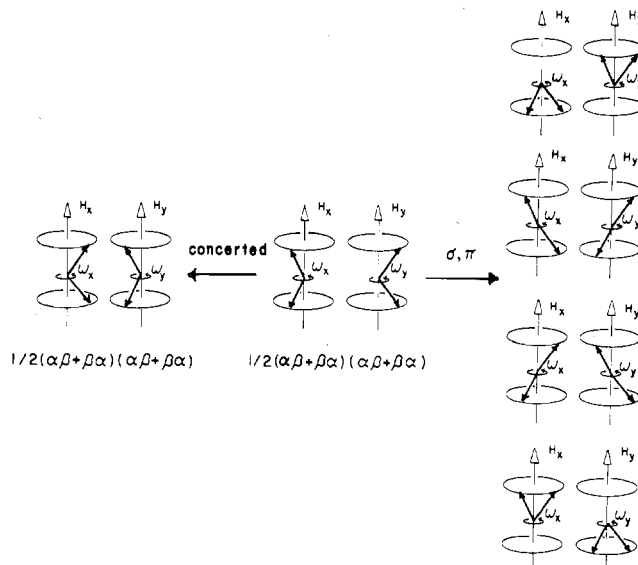


**Figure 5.** Classical representation of the influence of $\sigma,\pi$ and concerted interchange events on the proton spin configuration $\chi_{11} = {}^1/_2(\alpha\beta + \beta\alpha)(\alpha\beta + \beta\alpha)$.

by allowing $H_3$ and $H_4$ to interchange. Equation 18 permits $\alpha\beta\beta\alpha + \beta\alpha\alpha\beta$ to be set equal to $\phi_7-\phi_{10}$. The results of similar arguments applied to $\phi_8$, $\phi_9$, and $\phi_{10}$ are listed in Table I.

The difference between the classical and Kaplan procedures for determining the influence of the $\sigma,\pi$ mechanism on $\chi_7$–$\chi_{10}$ is unimportant in any practical sense in discussing the spectrum of tetra(*trihapto*allyl)zirconium at this simplest level of approximation: the spectra calculated for the $\sigma,\pi$ mechanism are insensitive to the transfer of magnetization between the four degenerate transitions making up the central line of the spectrum.[23,24] In instances in which these transi-

(23) It is worthwhile pointing out in this connection that the procedure described previously by us for calculating the dynamic ${}^{31}P$ nmr spectrum of $(CH_3)_2NPF_4$ is *formally* in error in its description of the exchange behavior of the central three lines, since the relative probabilities of magnetization transfer between transitions were obtained using the classical reasoning outlined here.[24] However, the correct probabilities (given in Table I of this paper) lead to a kinetic exchange matrix identical with that given previously,[24] and neither the line shapes nor the conclusions of that paper are altered by use of the correct probabilities obtained by the Kaplan procedure.
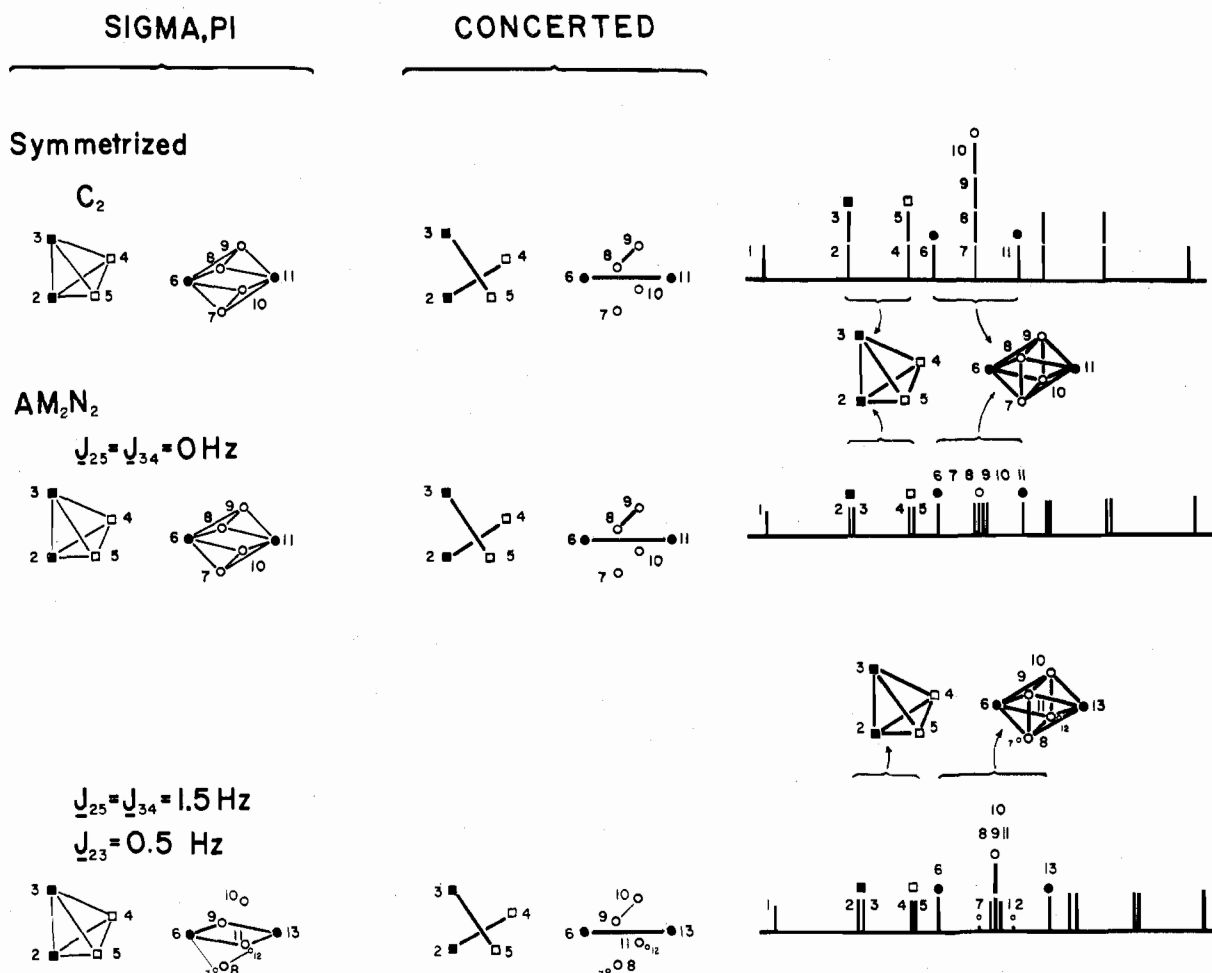
$$(\chi_7)_{\text{before}} = {}^1/_2(\alpha\beta + \beta\alpha)(\alpha\beta + \beta\alpha)$$

$$= {}^1/_2(\alpha\beta\alpha\beta + \alpha\beta\beta\alpha + \beta\alpha\alpha\beta + \beta\alpha\beta\alpha)]$$

$$\Big\downarrow \begin{array}{l}\text{interchange}\\ H_2 \text{ and } H_5\end{array}$$

$$\qquad\qquad (20)$$

$${}^1/_2(\beta\beta\alpha\alpha + \alpha\beta\beta\alpha + \beta\alpha\alpha\beta + \alpha\alpha\beta\beta)] =$$

$$(\chi_7)_{\text{after}} = {}^1/_2(\phi_6 + \phi_7 - \phi_{10} + \phi_{11})$$

**Figure 6.** Graphical representation of the rates of transfer of magnetization between transitions of $H_1$ of 5 by $\sigma,\pi$ and concerted interchange processes, summarized from K matrices calculated (a) for symmetrized wave functions, (b) by assuming zero magnitudes for the two- and four-bond couplings ($AM_2N_2$, $J_{25} = J_{34} = J_{23} = 0$), and (c) by using finite values for these couplings ($J_{25} = J_{34} = 1.5$ Hz, $J_{23} = 0.5$ Hz). The intensity of the indicated transitions is proportional to the area of the symbols ($\circ$, $\square$), at the apices of the polyhedra, and the rate of transfer of magnetization between these transitions is approximately proportional to the thickness of the lines forming the edges of the polyhedra.

tions are not degenerate or when the spectrum becomes second order by virtue of inclusion of small coupling constants (*vide infra*), the correct magnetization transfer probabilities must be used. There is no question that the probabilities obtained using the Kaplan procedure and listed in Table I are the correct ones; nonetheless, it is interesting that the description based on a purely classical description of nuclear magnetism fails only when applied to a problem requiring a quantum mechanical interpretation of a classical phase angle.[25]

The differences in the way magnetization is transferred between transitions 6–11 by the concerted and $\sigma,\pi$ mechanisms provides the basis for an experimental distinction between these classes of mechanisms. In the former mechanism, magnetization exchanges between the 6 and 11 transitions ($\beta\beta\alpha\alpha \rightleftharpoons \alpha\alpha\beta\beta$) but not between these transformations and any of the transitions 7–10 ($\alpha\beta \pm \beta\alpha$)($\alpha\beta \pm \beta\alpha$), which in turn exchange magnetization only among themselves. Thus, in going from slow- to fast-exchange spectra, the 6 and 11

(24) G. M. Whitesides and H. L. Mitchell, *J. Amer. Chem. Soc.*, **91**, 5384 (1969).

(25) Even here, the classical picture may contain the correct information if interpreted differently. In particular, note that the classical phase angles within the pairs formed by the interchange are necessarily equal, and in the limiting cases in which this angle is 0 and $\pi$ radians, the classical procedure leads to the same answer as the Kaplan procedure. The ambiguities in interpretation arise when this angle differs from 0 or $\pi$.
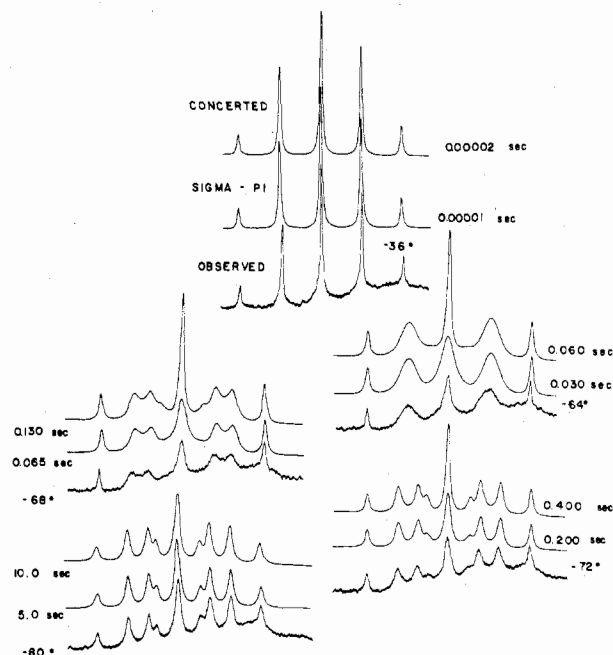


**Figure 7.** Comparison of the spectra observed for $H_1$ of 5 as a function of temperature in $CClF_3$ with spectra calculated based on symmetrized wave functions.

transitions should broaden and coalesce, while the line composed of the superimposed transitions 7–10 should remain sharp. In contrast, the entire group of transitions 6–11 is coupled by magnetization exchange in a $\sigma,\pi$ mechanism: all three of the lines observed for this group of transitions would be expected to broaden and coalesce in the region of intermediate exchange rates. Thus, although in either mechanism the three distinct lines made up of the central group of six transitions (6–11) are predicted qualitatively to coalesce to a single line in the fast-exchange limit, in a concerted mechanism the line composed of the superimposed 7–11 transitions should remain sharp throughout the region of intermediate exchange rates, while in a $\sigma,\pi$ mechanism this line should broaden.

To calculate line shapes based on the consideration outlined in this section, the coefficients of Table I are used directly (*cf.* eq 9a) to form a kinetic exchange matrix **K** (eq 9e). For example, for the crucial density matrix elements $\rho_6$–$\rho_{11}$, the appropriate submatrices of **K** for $\sigma,\pi$ and concerted mechanisms are given by eq 21 and 22.[26]

$$\tau(\mathbf{K}_{\sigma,\pi}) = \begin{array}{c} \\ 6 \\ 7 \\ 8 \\ 9 \\ 10 \\ 11 \end{array}\begin{array}{cccccc} 6 & 7 & 8 & 9 & 10 & 11 \\ \hline -1 & ^1/_4 & ^1/_4 & ^1/_4 & ^1/_4 & 0 \\ ^1/_4 & -^3/_4 & 0 & 0 & ^1/_4 & ^1/_4 \\ ^1/_4 & 0 & -^3/_4 & ^1/_4 & 0 & ^1/_4 \\ ^1/_4 & 0 & ^1/_4 & -^3/_4 & 0 & ^1/_4 \\ ^1/_4 & ^1/_4 & 0 & 0 & -^3/_4 & ^1/_4 \\ 0 & ^1/_4 & ^1/_4 & ^1/_4 & ^1/_4 & -1 \end{array} \quad (21)$$

$$\tau(\mathbf{K}_{\text{concerted}}) = \begin{array}{c} \\ 6 \\ 7 \\ 8 \\ 9 \\ 10 \\ 11 \end{array}\begin{array}{cccccc} 6 & 7 & 8 & 9 & 10 & 11 \\ \hline -1 & 0 & 0 & 0 & 0 & 1 \\ 0 & -1 & 0 & 0 & 1 & 0 \\ 0 & 0 & -1 & 1 & 0 & 0 \\ 0 & 0 & 1 & -1 & 0 & 0 \\ 0 & 1 & 0 & 0 & -1 & 0 \\ 1 & 0 & 0 & 0 & 0 & -1 \end{array} \quad (22)$$

Rather than consume space in writing out the full **K** matrices, we have adopted a graphical method of summarizing the information they contain (Figure 6). In this figure, a group of transitions is represented by the vertices of an appropriate polyhedron, and the relative magnitudes of the elements of the **K** matrix connecting these transitions are summarized by numbers beside each edge of the polyhedron. To assist in the qualitative assimilation of these data, circles or squares of area roughly proportional to the intensity of the indicated transition are located at each apex of the polyhedron, and the thicknesses of the lines along the edges are

(26) If desired, these matrices can be reduced to matrices of lower dimension by inspection, by noting that transitions 7–10 are degenerate and that they are characterized by identical rates of magnetization transfer to transitions 6 and 11. Thus, describing the behavior of the four superimposed transitions by a density matrix element which we will call $\rho_{7-10}$, eq 21 and 22 could be rewritten as

$$\tau(\mathbf{K}_{\sigma,\pi}) = \begin{array}{c} \\ 6 \\ 7\text{–}10 \\ 11 \end{array}\begin{array}{ccc} 6 & 7\text{–}10 & 11 \\ \hline -1 & 1 & 0 \\ ^1/_4 & -^1/_2 & ^1/_4 \\ 0 & 1 & -1 \end{array}$$

$$\tau(\mathbf{K}_{\text{concerted}}) = \begin{array}{c} \\ 6 \\ 7\text{–}10 \\ 11 \end{array}\begin{array}{ccc} 6 & 7\text{–}10 & 11 \\ \hline -1 & 0 & 1 \\ 0 & 0 & 0 \\ 1 & 0 & -1 \end{array}$$

These submatrices are identical with analogous expressions used in previous discussions of the spectrum of $(CH_3)_2NPF_4$.[24]
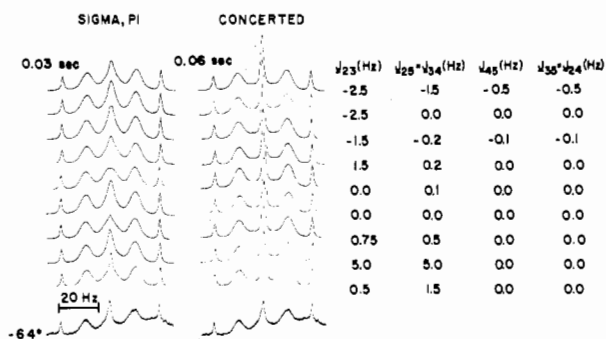


**Figure 8.** Spectra calculated for $H_1$ of **5** using a range of values of the two- and four-bond couplings $J_{25} = J_{34}$ and $J_{23}$; for the $\sigma,\pi$ mechanism, $\tau = 0.03$ sec; for the concerted mechanism, $\tau = 0.06$ sec.

| $J_{23}(\text{Hz})$ | $J_{25}=J_{34}(\text{Hz})$ | $J_{45}(\text{Hz})$ | $J_{35}=J_{24}(\text{Hz})$ |
|---|---|---|---|
| -2.5 | -1.5 | -0.5 | -0.5 |
| -2.5 | 0.0 | 0.0 | 0.0 |
| -1.5 | -0.2 | -0.1 | -0.1 |
| 1.5 | 0.2 | 0.0 | 0.0 |
| 0.0 | 0.1 | 0.0 | 0.0 |
| 0.0 | 0.0 | 0.0 | 0.0 |
| 0.75 | 0.5 | 0.0 | 0.0 |
| 5.0 | 5.0 | 0.0 | 0.0 |
| 0.5 | 1.5 | 0.0 | 0.0 |

made proportional to the magnitudes of the corresponding elements of **K** (that is, proportional to the rate constants for transfer of magnetization between the transitions connected by that edge); if an edge is omitted from the polyhedron, the magnitude of the corresponding element of **K** is zero. The **K** matrices for both $\sigma,\pi$ and concerted interchanges of **5** derived from the data of Table I are summarized by this figure by the polyhedra in the row labeled "symmetrized" wave functions.

Spectra were calculated using this **K** matrix and eq 10 for a range of values of $\tau$ for both concerted and $\sigma,\pi$ mechanisms. In this approximation, the frequencies of the transitions are read directly from the experimental spectra: the nuclear spin Hamiltonian is not used at any point in the calculations, since the coupling constants that influence the spectrum of $H_1$ appear only as frequency separations between resonances, and the chemical shifts between $H_1$ and $H_{2-5}$ are assumed to be large. Comparison of calculated and observed spectra (Figure 7) indicated two points of significance. First, spectra calculated using the **K** matrices generated using either mechanistic hypothesis are in qualitative agreement with the observed spectra in basic structure; *viz*, transitions 1 and 16 remain sharp throughout the exchange-broadened region; transitions 2,3 and 4,5 (and 12,13 and 14,15) coalesce to single lines; transitions 6–11 coalesce to a single line. Second, although the spectra calculated assuming a $\sigma,\pi$ mechanism appear to be in closer agreement with the observed spectra than were those calculated assuming a concerted mechanism, *neither* set of calculated spectra is in fact in satisfactory agreement with the experimental spectra for the important transitions 6–11. In particular, the calculated line shapes for the superimposed 7–10 transitions in the $\sigma,\pi$ mechanism show uniform broadening of each of the component transitions, as expected from eq 21–22 (or Figure 6), while the corresponding central feature of the fast-exchange experimental spectrum appears to be made up of at least two components that broaden at appreciably different rates as the temperature is lowered. This disagreement between experimental and calculated spectra precludes a reliable decision between mechanisms at this level of discussion and forces consideration at a less approximate (and less readily physically interpretable) level.

**Calculations Based on $AM_2N_2$ Nuclear Spin Wave Functions.** A possible origin of the disagreement between the experimental spectra and those calculated in the previous section lay in the assumption that the symmetrized wave functions for four nuclei with $C_2$ symmetry (Figure 1) provided an approximation to the eigenfunctions of the nuclear spin Hamiltonian adequate for the prediction of dynamic line shape behavior. In principle, the finite chemical shift
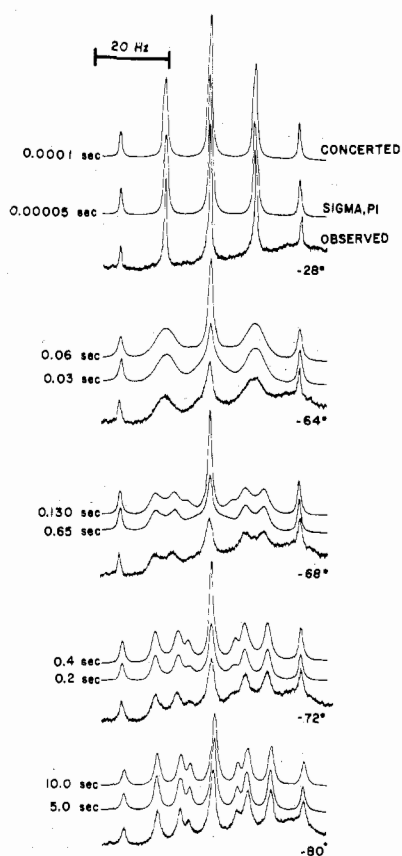
**Figure 9.** Comparison of the spectra observed for $H_1$ of **5** as a function of temperature in $CCl_3F$ with spectra calculated using $J_{23} = 0.5$ Hz, $J_{25} = J_{34} = 1.5$ Hz.

differences between the nuclei of **5** might result in mixing of those wave functions $\chi$ of Figure 1 having the same symmetry and same value of $F_z$ and, in consequence, alter the relatively simple magnetization exchange scheme obtained using these symmetrized functions. This point was easily checked by calculating the eigenfunctions of the spin Hamiltonian using appropriate parameters (*viz.*, $\delta\nu_{12} = \delta\nu_{13} = 192$ Hz, $\delta\nu_{14} = \delta\nu_{15} = 334$ Hz, $J_{12} = J_{13} = 9.3$ Hz, $J_{14} = J_{15} = 15.9$ Hz, and $J_{23} = J_{24} = J_{25} = J_{34} = J_{45} = 0$), combining these wave functions with eq 8, 9c, and 9d to generate **K** matrices, and solving the resulting line shape equations (eq 10) to produce calculated spectra. The effect on the static spectrum of introducing these chemical shifts and coupling constants is to split certain degenerate transitions. Nevertheless these **K** matrices (summarized in Figure 6 in the column labeled $AM_2N_2$) and the resulting calculated spectra were indistinguishable from those obtained using only the symmetrized wave functions. Thus, the amount of mixing of wave functions introduced by using "real" chemical shifts is too small to have a significant effect on the spectra.

The remaining assumption that might be responsible for the calculation of incorrect line shapes concerns the coupling constants: only the three-bond vicinal couplings $J_{12} = J_{13}$ and $J_{14} = J_{15}$ were assumed nonzero in the calculations discussed to this point. Although the experimental spectrum contains no evidence of other couplings, the resolution in these spectra is not particularly good, and small coupling would not be readily detectable. To investigate the possible influence of small two- and four-bond couplings on spectral line shapes, $J_{23}$ and $J_{25} = J_{34}$ were varied independently through values ranging in magnitude from +2.5 to −2.5 Hz, and line shapes calculated as described previously from the
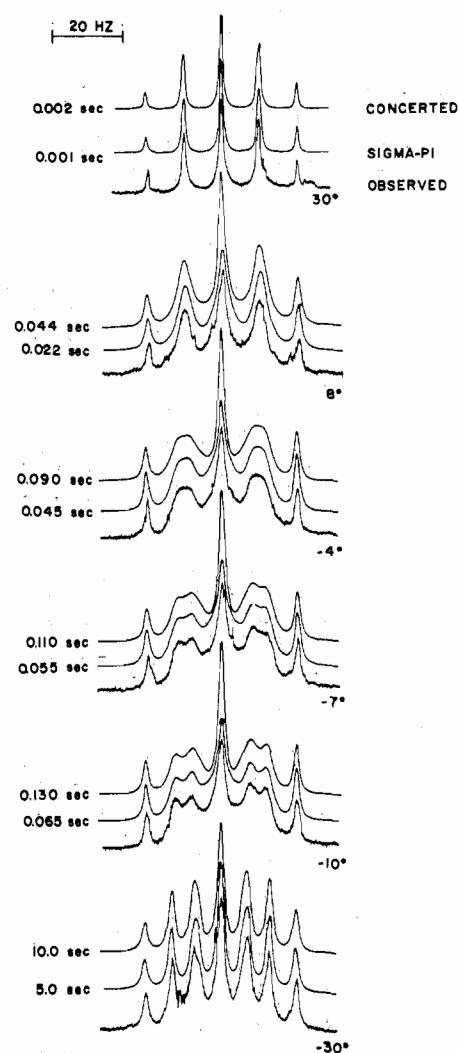


**Figure 10.** Comparison of calculated and observed spectra for $H_1$ of chloro(*trihapto*allyl)palladium(II) dimer in DMSO-$d_6$.

resulting eigenfunctions and **K** matrices.[27] The principal effects of introducing small nonzero values for these couplings on the slow-exchange spectra are the production of small splittings between transitions that are degenerate when these couplings are zero and the introduction of additional

(27) Introduction of $J_{45} \leqslant 0.2$ Hz and $J_{24} = J_{35} \leqslant 0.2$ Hz in combination with various sets of $J_{25} = J_{34}$ and $J_{23}$ had little effect on the calculated line shapes of exchange-broadened spectra. Although magnitudes of these small couplings have been reliably established in relatively few cases, the ranges used here are in line with available data. The majority of cited coupling constants have been obtained for substituted allyl moieties.[3,4,6,9,28,29] The magnitudes of the coupling constants in 1,3-butadieneiron tricarbonyl (iii) have been

iii
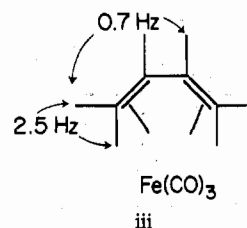
determined by double resonance studies and verified by computer simulation.[30]

(28) M. S. Lupin and B. L. Shaw, *Tetrahedron Lett.*, 883 (1964).

(29) J. W. Faller, C. Chen, M. J. Mattina, and A. Jakutowski, *J. Organometal. Chem.*, in press.

(30) H. G. Preston and J. C. Davis, *J. Amer. Chem. Soc.*, **88**, 1585 (1966).

low-intensity transitions in the spectrum (Figure 6). The practical influence of these couplings on the line shapes calculated in the intermediate-exchange region assuming a $\sigma,\pi$ mechanism is that of yielding a central spectral feature apparently composed of superimposed components having different widths and different rates of broadening. A number of combinations of magnitudes and signs of these couplings yielded calculated spectra in reasonable qualitative agreement with the observed spectra: a selection of these calculated spectra is shown in Figure 8, together with the spectrum observed at $-64°$, at which temperature the deviation of the shape of the central line from that characteristic of a single transition was most pronounced. The values selected for use in fitting line shapes over the entire temperature region are those of the lowermost of the calculated spectra in this figure: $J_{23} = 0.5, J_{25} = J_{34} = 1.5$ Hz. The relative insensitivity of the line shapes to the magnitudes of these couplings is such that these values cannot be claimed to be highly accurate; in fact, rather different values might give closer agreement between calculated and observed spectra. Nevertheless, two points are of central concern to this paper. First, the introduction of small, physically reasonable, values for these couplings is required to yield calculated line shapes based on the $\sigma,\pi$ mechanism that are in close agreement with the observed line shapes. Second, *no* combination of coupling constants could be found that would bring spectra calculated assuming the concerted mechanism into agreement with the observed spectra (Figure 8). We conclude from the good agreement obtained between the observed spectra and those calculated using these coupling constants over the complete range of dynamic line shape behavior (Figure 9) that the reaction responsible for the interchange of syn and anti protons in tetra(*trihapto*allyl)zirconium(IV) is characterized by the permutational properties that characterize a $\sigma,\pi$ process.

For comparison, we examined briefly the line shape behavior of chloro(*trihapto*allyl)palladium(II) dimer, a compound established previously to interchange syn and anti protons by a $\sigma,\pi$ process (Figure 10).[3] Although line shapes in this system appeared less sensitive to the magnitudes of the small couplings than did those of **5**, agreement between observed and calculated spectra could again be obtained only assuming a $\sigma,\pi$ mechanism and this agreement appeared to be improved by the introduction of nonzero values for $J_{25} = J_{34}$. Figure 11 compares line shapes calculated assuming a $\sigma,\pi$ mechanism for proton interchange for two values of the four-bond syn-syn coupling: $J_{25} = 0, J_{25} = 1.0$ Hz; the experimental spectrum obtained at $-4°$ seemed to provide the clearest indication of multiple components characterized by different widths for the central feature.[31]

### Conclusions

The data presented in this paper establish that the predominant reaction responsible for the interchange of the syn and anti protons of tetra(*trihapto*allyl)zirconium (**1**) in CFCl$_3$ solution is one characterized by anticorrelated motions at the two ends of the allyl moiety, *viz.*, in all probability by a $\sigma,\pi$ mechanism, although neither a mechanism of the type represented by eq 2 nor other mechanisms characterized by the same type of nuclear permutation scheme can be excluded using these kinds of data. The quality of the spectra is such



**Figure 11.** The influence of the magnitude of $J_{25} = J_{34}$ on spectra calculated for H$_1$ of chloro(*trihapto*allyl)palladium(II) dimer based on a $\sigma,\pi$ mechanism.

that it would not be possible to detect a small contribution to the line shapes due to these excluded mechanisms.

Comparisons of calculations for the spin system of **5** carried out at several levels at completeness suggest a point of concern for similar future calculations. Consideration of the behavior of this moderately complex, coupled spin system at a simple classical level is sufficient to predict the broad features of the line shape behavior; however, certain small spin–spin couplings can have a pronounced effect on the broadening observed for individual lines in the intermediate-exchange region, and careful consideration of the influence of small couplings clearly must be included in any calculation which requires a close fit between observed and calculated spectra.

### Experimental Section

**General Methods.** Reactions involving organometallic compounds were carried out under atmospheres of prepurified nitrogen using standard techniques for manipulation of air- and water-sensitive compounds.[32]

All nmr spectra were run on a Varian HA-100IL spectrometer equipped with a Varian V-6040 variable-temperature unit. A Digitek digital thermocouple was used to measure the temperature of the sample in the probe.

**Allylmagnesium bromide** was prepared according to the procedure

(31) K. C. Ramey and G. L. Straton, *J. Amer. Chem. Soc.*, **88**, 4387 (1966), report $J_{25} < 1$ Hz for chloro(*trihapto*allyl)palladium dimer. We have found that a variety of slow-exchange spectra calculated assuming a peak width at half-height of 0.8 Hz, Lorentzian line shapes, and coupling constants as large as $J_{23} = 1.5$ Hz and $J_{25} = 1.0$ Hz are all essentially indistinguishable.
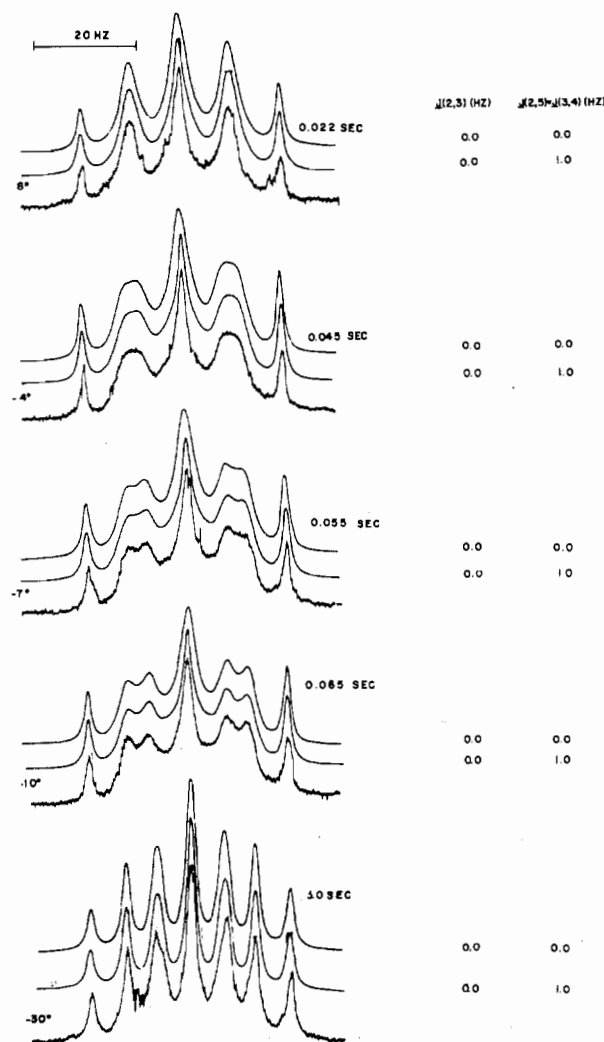
(32) D. F. Shriver, "The Manipulation of Air-Sensitive Compounds," McGraw-Hill, New York, N. Y., 1967, Chapter 7.

of Grummit, Budewitz, and Chudd.[33]  To 6.0 g (260 mg-atom) of magnesium powder (40 mesh) in *ca.* 125 ml of ether, freshly distilled from lithium aluminum hydride, in a flame-dried 300-ml round-bottomed flask equipped with magnetic stirrer, condenser, and No-Air stopper, was added at 0° *ca.* 0.5 ml of 1,2-dibromoethane.  To the activated magnesium, 7.0 g (58 mmol) of freshly distilled allyl bromide was added at 0° over a 2-hr period.  The solution was allowed to stir at 0° for an additional 5 hr and was transferred by cannula to a flame-dried 200-ml storage bottle.  The residual salts were washed with *ca.* 20 ml of ether, and the washings transferred to the storage bottle and mixed thoroughly.  Titration with 0.105 *M* sec-butyl alcohol in xylene using 1,10-phenanthroline[34] as indicator showed the solution to be 0.36 *M*.

Tetra(*trihapto*allyl)zirconium(IV) (5) was prepared according to the procedure of Becconsall, Job, and O'Brien.[7]  In a 100-ml round-bottomed flask was placed 0.79 g (3.9 mmol) of zirconium tetrachloride.  To the salt, cooled to −60°, 40 ml of 0.30 *M* (12.0 mmol) allylmagnesium bromide was added over a 1.5 hr period.  The mixture was stirred for 20 hr at external temperature of *ca.* −70° (Dry Ice–isopropyl alcohol) and filtered at *ca.* −40° through a Celite pad, which previously had been dried with *ca.* 2 ml of *n*-butyllithium.  The solvent was removed under vacuum while maintaining the sample temperature between −40 and −30°.

Preparation of Nmr Samples of 5.  *Ca.* 5 ml of fluorotrichloromethane, previously degassed by three freeze–thaw cycles, was distilled into the storage tube containing the red solid 5, obtained by removal of ether under vacuum at −78° (Dry Ice–isopropyl alcohol).  An aliquot of the resulting solution was transferred at −78° through a stainless steel cannula into an nmr tube, adapted with a 12/15 ball

joint and joined to a vacuum stopcock, fitted with a No-Air stopper.  TMS internal standard was added and the tube sealed under vacuum.  The sample used showed no absorption in the nmr spectrum due to ether, but did show a broad impurity peak centered slightly upfield from the H₁ resonances of 5.  The nature of this impurity was not explored.  Extensive decomposition was observed if the sample was not stored below −20°.

*Trihapto*allylpalladium chloride dimer was prepared by Dr. D. L. Tibbets.  The nmr sample used in this study was prepared by adding 75 mg (0.206 mmol) of the palladium complex and 64.5 mg (0.826 mmol) of dimethyl sulfoxide-$d_6$ (2 equiv of DMSO-$d_6$/allyl group) to 0.5 ml of a 10% solution of benzene in deuteriochloroform.

Calculations were performed at the Massachusetts Institute of Technology Information Processing Center using the program EXCHSYS[15,35] to compute eigenfunctions and line shapes of static spectra, K matrices, and interchange-broadened line shapes.

**Registry No.**  Tetra(*trihapto*allyl)zirconium(IV), 12090-34-5; chloro(*trihapto*allyl)palladium(II) dimer, 12012-95-2.

(33) O. Grummit, E. P. Budewitz, and C. C. Chudd, "Organic Syntheses," Collect. Vol. IV, Wiley, New York, N. Y., 1963, p 748.

(34) S. C. Watson and J. F. Eastham, *J. Organometal. Chem.,* 9, 165 (1967).

(35) EXCHSYS is based on the program LAOCN3:  A. A. Bothner-By and S. M. Castellano, in D. F. deTar, "Computer Programs for Chemistry," Vol. I, W. A. Benjamin, New York, N. Y., 1968, and local line shape programs, KMATRX and EXCNMR, written by J. B. Lisle, C. P. Powell, J. K. Krieger, and G. M. Whitesides.

---

# Structural Studies in Main-Group Chemistry.  IV.[1]  *O*-Trialkyltin Hydroxylamines[2]

PHILIP G. HARRISON

The organotin hydroxylamine derivatives Me₃SnONEt₂, R₃SnONHCOPh (R = Me, *n*-Pr), and R₃SnONPhCOPh (R = Me, *n*-Pr, Ph) and the organosilicon and organolead analogs Me₃SiONPhCOPh and Ph₃PbONPhCOPh have been synthesized.  All are inert to hydrolysis save Me₃SnONEt₂, which readily reverts to its protic precursors in air, and monomeric in solution (osmometry).  Attempts to prepare Ph₃SnONHCOPh from triphenyltin hydroxide result in the formation of tetraphenyltin in high yield, and from triphenyltin chloride and excess triethylamine the ionic species (NEt₃H⁺)(Ph₃SnONCPhO⁻ is produced.  The trimethyltin homolog of the latter is prepared by dissolution of Me₃SnONHCOPh in triethylamine.  The structures of the derivatives in both solution and solid phases are discussed in terms of their infrared, nuclear magnetic resonance, tin-119m Mossbauer, and mass spectra.  The stability of the tin and lead derivatives is due to the increase of the coordination number at the metal atom *via* *intra*molecular coordination of the carbonyl group to the metal.  The mass spectra for Me₃SnONHCOPh and Me₃SnONPhCOPh indicate the presence of associated, most probably weakly associated dimer, species in the solid.  High-resolution mass measurements have confirmed the presence of the SnOSn backbone in the more abundant ditin fragments and also the composition of monotin fragments, among which are some which arise from novel ring contraction reactions involving the elimination of oxygen or phenylnitrene from MONPhCPh=O heterocyclic species.  The major fragmentation processes of Me₃SiONPhCOPh have been corroborated by the observation of metastable ions and involve mainly the formation of phenyl-containing ions in which the charge may be effectively delocalized.

## Introduction

The synthesis and properties of main-group metal and metalloid derivatives containing the M–O–N linkage continues to arouse much interest.[3,4]  Oxime derivatives of lithium,[3]

silicon, germanium, tin,[3,4] lead, arsenic, and antimony[4] have previously been synthesized by us, while attempts to prepare similar phosphorus derivatives led to the formation of phosphorylamines *via* an Arbuzov rearrangement.[4]  The *O*-(trialkylstannyl)oximes[3] are volatile monomeric liquids except for cyclohexanone *O*-(trimethylstannyl)oxime, for which infrared, tin-119m Mossbauer, and high-resolution mass spectral data indicated association *via* distannoxane SnOSnO ring formation in the solid.  Such association is however rather weak since only monomeric species could be

(1) Part III:  P. G. Harrison and J. J. Zuckerman, *J. Organometal. Chem.,* in press.

(2) A preliminary communication has appeared:  P. G. Harrison, *J. Organometal. Chem.,* 38, C5 (1972).

(3) P. G. Harrison and J. J. Zuckerman, *Inorg. Chem.,* 9, 175 (1970), and references therein.

(4) P. J. Harrison and J. J. Zuckerman, *Inorg. Nucl. Chem. Lett.,* 6, 5 (1970), and references therein.